ORIGINAL ARTICLE

Accuracy of 64-slice CT angiography for the detection of functionally relevant coronary stenoses as assessed with myocardial perfusion SPECT

**Oliver Gaemperli · Tiziano Schepis · Pascal Koepfli ·
Ines Valenta · Jan Soyka · Sebastian Leschka ·
Lotus Desbiolles · Lars Husmann · Hatem Alkadhi ·
Philipp A. Kaufmann**

Abstract

Purpose CT angiography (CTA) offers a valuable alternative for the diagnosis of CAD but its value in the detection of functionally relevant coronary stenoses remains uncertain. We prospectively compared the accuracy of 64-slice CTA with that of myocardial perfusion imaging (MPI) using ^{99m}Tc-tetrofosmin-SPECT as the gold standard for the detection of functionally relevant coronary artery disease (CAD).

Methods MPI and 64-slice CT were performed in 100 consecutive patients. CTA lesions were analysed quantitatively and area stenoses ≥50% and ≥75% were compared with the MPI findings.

Results In 23 patients, MPI perfusion defects were found (12 reversible, 13 fixed). A total of 399 coronary arteries and 1,386 segments was analysed. Eighty-four segments (6.1%) in 23 coronary arteries (5.8%) of nine patients (9.0%) were excluded owing to insufficient image quality. In the remaining 1,302 segments, quantitative CTA revealed stenoses ≥50% in 57 of 376 coronary arteries (15.2%) and stenoses ≥75% in 32 (8.5%) coronary arteries. Using a cut-off at ≥75% area stenosis, CTA yielded the following sensitivity, specificity, negative (NPV) and positive predictive value (PPV), and accuracy for the detection of any (fixed and reversible) MPI defect: by patient, 75%, 90%, 93%, 68% and 87%, respectively; by artery, 76%, 95%, 99%, 50% and 94%, respectively.

Conclusion Sixty-four-slice CTA is a reliable tool to rule out functionally relevant CAD in a non-selected population with an intermediate pretest likelihood of disease. However, an abnormal CTA is a poor predictor of ischaemia.

Keywords Coronary CT angiography ·
Myocardial perfusion imaging · SPECT ·
Coronary artery disease

O. Gaemperli · T. Schepis · P. Koepfli · I. Valenta · J. Soyka ·
P. A. Kaufmann (✉)
Nuclear Cardiology, Cardiovascular Center,
University Hospital Zurich NUK C 40,
Raemistrasse 100,
8091 Zurich, Switzerland
e-mail: pak@usz.ch

S. Leschka · L. Desbiolles · L. Husmann · H. Alkadhi
Institute of Diagnostic Radiology, University Hospital Zurich,
Zurich, Switzerland

P. A. Kaufmann
Zurich Center for Integrative Human Physiology (CIHP),
University of Zurich,
Zurich, Switzerland

Introduction

In 2003 about 2 million invasive coronary angiography (CA) procedures were performed in Europe [1]. In spite of continuous improvements in CA to minimise the risks inherent in invasive testing, the associated economic burden, the inconvenience to patients and the remaining risk of severe complications have prompted an intensive search for alternative, non-invasive means for coronary artery imaging [2]. Since 1999, multislice spiral computed tomography (MSCT) systems with simultaneous acquisition of four or more slices and gantry rotation times of less than half a second have been available [3]. Compared with CA, multislice CT angiography (CTA) has delivered promising results regarding accuracy in the detection and

validation of coronary lesions. Particularly scanners with 16 or 64 slices and a faster gantry rotation have been shown to reduce motion artefacts and blooming artefacts related to partial volume effects in cases of heavy calcifications, although both types of artefact remain important limitations of cardiac CT in clinical routine use [4–13]. However, the diagnostic value of CTA in detecting functionally relevant coronary stenoses as defined by reversible or fixed perfusion defects on myocardial perfusion imaging (MPI) remains uncertain as only limited data are available on this specific issue [4, 14].

MPI using single-photon emission computed tomography (SPECT) is a widely established method for the non-invasive assessment of coronary artery disease (CAD) [15]. In addition to its diagnostic accuracy, SPECT allows evaluation of the functional significance of coronary stenoses and provides useful prognostic information for cardiac risk stratification [16–19]. By contrast, the purely anatomical information depicted by invasive and non-invasive angiography offers limited functional and prognostic data on which clinical decision-making can be based [20]. In fact, patients with documented CAD but normal MPI are at low risk for major cardiac events, comparable to that in patients without significant CAD [21].

Thus, the aim of the present study was to compare the accuracy of 64-slice CTA with that of MPI for the detection and validation of functionally significant coronary lesions.

Materials and methods

Study population

The study was conducted prospectively, enrolling 100 consecutive patients who were referred to our department for MPI for clinical indications. A subgroup of the study population is shared with a recent study on left ventricular volumes [22]. They underwent 64-slice CTA within 1 month of the MPI. Reasons for patient's referral were typical or atypical chest pain, pathological tread mill test, dyspnoea or syncope. Patients were excluded from the study if they had cardiac arrhythmia, impaired renal function, known intolerance of iodinated contrast medium or coronary interventions between the two examinations. The study protocol had been approved by the local ethics committee and all patients gave written informed consent for the CT scan before the study.

Myocardial perfusion imaging

All patients underwent a 1-day electrocardiographically (ECG)-gated stress/rest MPI protocol with pharmacological stress using a dose of at least 300 MBq of ^{99m}Tc-tetrofosmin at peak pharmacological stress and 900 MBq at rest at least 1 h after the first injection. Pharmacological stress test was performed with a 7-min infusion of adenosine at a standard rate of 140 μg kg^{-1} min^{-1} and the stress dose of ^{99m}Tc-tetrofosmin was injected 3 min into the pharmacological stress [23]. Patients were told to refrain from caffeine-containing beverages for at least 12 h, from nitrates for 24 h, and from beta-blockers for 48 h before the MPI study.

Gated SPECT studies were acquired with a dual-head detector camera (Millennium VG & Hawkeye, General Electric Medical Systems, Milwaukee, WI, USA); a low-energy, high-resolution collimator; a 20% symmetric window at 140 keV; a 64×64 matrix; an elliptical orbit with step-and-shoot acquisition at 3° intervals over 180°; and a 20-s dwell time per stop. Acquisitions were gated at 16 frames per R-R cycle with a 50% window of acceptance. For all patients, the summed non-gated SPECT image set was reconstructed on a dedicated workstation (eNTEGRA or Xeleris, GE Medical Systems, Milwaukee, WI, USA), using an iterative reconstruction algorithm (OSEM, ordered-subset expectation maximisation with two iterations and ten subsets) with X-ray based attenuation correction as previously reported [24, 25], into short axis, vertical long axis and horizontal long axis slices encompassing the entire left ventricle. In addition, polar maps of perfusion, wall motion and wall thickening were produced using a commercially available software package (Cedars QGS/QPS; Cedars-Sinai Medical Center, Los Angeles, CA, USA [26]), yielding semiquantitative perfusion scores at rest (SRS, summed rest score) and after stress (SSS, summed stress score). The summed difference score (SDS) was calculated as the difference of the previous two and used as an indicator of reversible perfusion abnormalities.

SPECT image interpretation was visually performed by consensus of two experienced nuclear cardiologists on short axis, horizontal long axis and vertical long axis slices, and semiquantitative polar maps of perfusion as previously reported [27]. Defects in the anterior and septal wall were allocated to the left anterior descending coronary artery (LAD), defects in the lateral wall to the left circumflex coronary artery (LCX) and inferior defects to the right coronary artery (RCA). In the watershed regions, allocation was determined according to the main extension of the defect onto the lateral, anterior or inferior wall. Reversible perfusion defects were considered myocardial ischaemia. Fixed perfusion defects with concomitant regional wall motion abnormalities were considered myocardial scars.

Sixty-four-slice CTA

The CTA images were acquired with a 64-detector CT scanner (General Electrics LightSpeed VCT, Milwaukee,

WI, USA) with a collimation of 64×0.625 mm and a total z-axis coverage of 40 mm. The minimal gantry rotation time was 0.35 s, the tube voltage was 120 kV, the tube current ranged from 280 to 750 mA using ECG modulation (i.e. reduction to about 40% of nominal tube current during systole to mid-diastole), and the pitch ranged from 0.18 to 0.26 depending on the patient's heart rate, resulting in a isotropic voxel resolution of 0.35 mm and temporal resolution of 87–175 ms. After two localisation scans, a low-dose native scan of the heart was performed for coronary calcium detection and scoring as previously reported [28]. Test bolus tracking with 15 ml of non-ionic contrast agent (Ultravist® 370 mg/ml, Schering AG, Berlin, Germany) was applied to calculate the exact arrival time of contrast agent in the coronary arteries, with a region of interest in the proximal part of the ascending aorta. A bolus of 70–100 ml of contrast agent was continuously injected into an antecubital vein (50–80 ml at 5.0 ml/s, then 20 ml at 3.5 ml/s) followed by a saline chaser bolus of 50 ml at a flow rate of 3.5 ml/s. Thereafter scanning was initiated, covering the distance from the tracheal bifurcation to the diaphragmatic side of the heart during a single inspiratory breath hold for an acquisition time of 5–7 s. Motion artefacts can be avoided by scanning at low heart rates [29–31]; therefore all patients with heart rates of >70 beats per minute (bpm) were pretreated intravenously with 5–10 mg of metoprolol tartrate (Lopresor®, Sankyo Pharma AG, Switzerland) directly before the scan according to our practice in daily clinical routine. For optimal heart phase selection, retrospective ECG gating was used. Retrospective reconstruction of the image data was performed for acquisition of phase images starting from early systole (5% of the R-R interval) and ending at late diastole (95% of the R-R interval) using 10% increments. All images were reconstructed with a display field of view of 25 cm, a standard soft tissue filter as suggested by the manufacturer and an effective slice thickness of 0.625 mm at an increment of 0.625 mm.

The CTA datasets were analysed using axial source images, multiplanar reformations (MPR) and thin-slab maximum intensity projections (MIP). All patients were evaluated by the same reader. Image quality was graded as excellent (no motion artefacts present), good (minor motion artefacts present), moderate (substantial motion artefacts present, but luminal assessment of significant stenoses still possible), heavily calcified (vessel lumen obscured by calcifications) or blurred (only contrast visualisation inside the vessel possible). Only excellent, good or moderate quality was considered acceptable for reliable image interpretation. Coronary arteries were assessed according to a 15-segment model proposed by the American Heart Association [32]. Each bypass graft was counted as an additional segment. In arteries with bypass grafts the

corresponding coronary artery was considered as patent if the bypass graft was patent. In segments containing a stent, the lumen could only be assessed if the stent diameter was larger than 2 mm, because smaller stents suffered from significant blooming artefacts caused by the stent material and could not be evaluated reliably. Blurred and heavily calcified segments were excluded from further analysis. In the remaining coronary segments, stenoses were quantitatively assessed as described previously by Leber et al. [11] (Fig. 1).

In brief, the average diameter was obtained from two orthogonal MIP-reconstructed image planes to calculate the cross-sectional area. Then, the area stenosis was determined by dividing the minimal luminal area of the stenotic segment by the area of adjacent non-stenotic reference vessel. A cut-off of (a) 50% area [4] and (b) 50% diameter stenosis [9, 10, 12, 13] resulting in a 75% area stenosis was
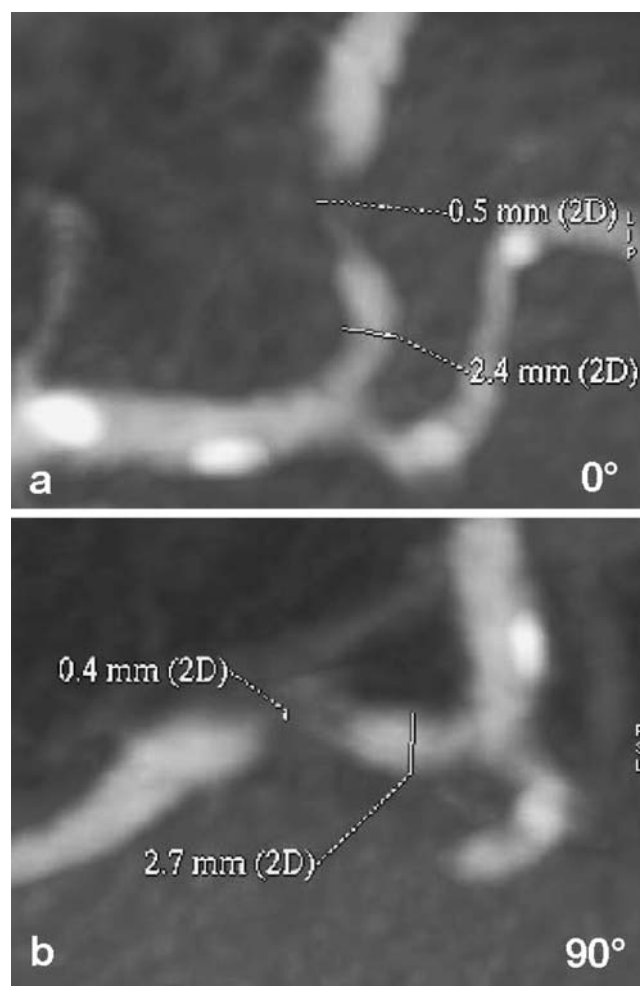

Fig. 1 Quantitative assessment of coronary stenoses on two longitudinal thin-slab MIPs. For three-dimensional evaluation of stenosis, minimal luminal diameter and reference diameter were measured in two different rotational planes at 0° (**a**) and 90° (**b**). The values in degrees refer to rotation of MIP planes around an axis along the vessel's centre line

used for classification of significant coronary stenoses and comparison with the MPI results.

Data interpretation and statistical analysis

In a second step, data from 64-slice CT images and MPI images were compared. Since assignment of single coronary segments on CT images to myocardial territories on MPI is not feasible, data analysis was performed on a per artery basis [LAD, LCX, RCA and left main artery (LMA)] as previously reported [4]. We also added per patient analysis as this provides the clinically most meaningful information for patient management. Both analyses were separately performed for stenoses ≥50% and ≥75%. In patients who had previously undergone coronary artery bypass grafting (CABG) and showed occluded or highly stenotic native coronary arteries, a specific coronary artery was only considered stenotic if the corresponding bypass graft showed a significant stenosis too.

Quantitative data are expressed as mean±SD. Quantitative values were compared using the two-sided Student's t test. Qualitative data are given in proportions and are compared using the chi-squared test. A p value <0.05 was considered statistically significant. Sensitivity, specificity, negative predictive value (NPV), positive predictive value (PPV) and accuracy were calculated for both lesion degrees as mentioned above. Accuracy was determined as the percentage of correct diagnoses in the entire sample [33].

Results

A hundred patients with a mean age of 61±11 years (range 38–86 years) were included in our analysis. Patient characteristics are summarised in Table 1. Considering all patients, CTA was performed within a mean interval of 3 days (range 0–30 days) from the MPI study; 79 patients had the CT scan performed on the same day as the MPI study.

CTA results

All patients were in stable sinus rhythm, and mean heart rate during CT was 61±8 bpm (range 43–83 bpm). Intravenous metoprolol tartrate (5–10 mg) was administered to 30 patients with heart rates >70 bpm at rest without any side-effects. A total amount of 103±24 ml of non-ionic contrast agent, including the 15 ml bolus of contrast agent used for bolus tracking, was injected without serious adverse events.

Image quality was excellent in 27 of 100 patients, good in 49 patients and moderate in 14 patients. In five patients CTA images were heavily calcified, and in the remaining five patients image quality was poor, mainly owing to

Table 1 Patient characteristics (n=100)

Characteristics	
Age (yrs)	61±11
Female gender	30
Weight (kg)	82±18
Height (cm)	169±16
Medical history	
Single-vessel coronary disease	5
Two-vessel coronary disease	7
Three-vessel coronary disease	5
Previous myocardial infarction	6
Previous PCI	14
Previous CABG	4
Left ventricular ejection fraction (%)	62±11
Cardiovascular risk factors	
Diabetes mellitus	14
Hypertension	58
Dyslipidaemia	48
Current smokers	34

PCI percutaneous coronary intervention, *CABG* coronary artery bypass grafting

motion artefacts; in these five patients the CTA image sets were classified as blurred.

A total of 1,386 coronary segments in 399 main coronary arteries (one patient was without an LMA owing to separate origin of the LAD and LCX) were analysed, including 12 aorto-coronary bypass grafts [four left internal mammary arteries, one right internal mammary artery (RIMA) and seven saphenous vein grafts] in four patients who had previously undergone CABG surgery.

Forty-one segments (3.0%) were not evaluable because of significant motion artefacts. The mean heart rate during scanning in these patients was significantly elevated compared with the rest of patients [67±7 vs 60±7 bpm (p=0.002)]. Forty-three segments (3.1%) were rated as heavily calcified or had intracoronary stents <2.0 mm in diameter with significant blooming artefacts preventing reliable luminal assessment. Coronary calcium score (CCS) in the entire group of patients was 505±813 (range 0–3,640) Agatston score equivalents (ASE). CCS was significantly higher in patients with calcified segments that had to be excluded from analysis than in the rest of the patients [1,407±1,176 vs 265±455 ASE (p<0.001)]. Overall, vessel diameter could not be evaluated for 84 of 1,386 segments (6.1%) in 23 of 399 coronary arteries (5.8%), representing nine of 100 patients (9.0%).

Quantitative CTA revealed area stenoses ≥50% in 109 of 1,302 segments (8.4%). In segments with a diameter <1.5 mm, quantitative assessment was deemed to be inaccurate and, therefore, 12 stenosed segments were excluded from further analysis. Thus, in the remaining 1,290 segments, quantitative CTA revealed stenoses in 97 segments (7.5%), corresponding to 57 of 376 coronary

arteries (15.2%) in 36 out of 91 patients (39.6%). Forty-two of these stenotic segments were located in the LAD, 23 in the LCX, 27 in the RCA territory and one in the LMA. Four stenotic lesions were located in aorto-coronary bypass grafts, which were found to be occluded on CTA (one RIMA and three vein grafts). The mean degree of stenosis as assessed by quantitative CTA was 84±14% area stenosis.

When applying a cut-off of 75% for significant stenoses, 60 segments (4.6%) were identified as stenotic by quantitative CTA, corresponding to 32 coronary arteries (8.5%) in 22 patients (24.2%). Twenty-two stenotic segments were located in the LAD, 12 in the LCX and 22 in the RCA territory. Four stenotic segment belonged to the aorto-coronary bypass grafts mentioned above. The mean degree of stenosis in segments with stenoses ≥75% as assessed by quantitative CTA was 93±8%.

MPI results

MPI was successfully performed in all 100 patients and all image data sets were amenable to image interpretation. Visual image analysis revealed 12 reversible and 13 fixed perfusion defects in 23 out of 100 patients. One patient showed both fixed and reversible perfusion defects and another showed two fixed defects. All the fixed perfusion defects showed concomitant regional wall motion abnormalities. Of the 12 reversible perfusion defects, seven were

located in the LAD, two in the LCX (Fig. 2) and three in the RCA territory. Of the 13 fixed perfusion defects, five were located in the LAD, one in the LCX (Fig. 3) and seven in the RCA territory. Seventy-seven patients showed no perfusion abnormalities on MPI. All summed perfusion scores were significantly higher in patients with abnormal MPI than in patients with normal MPI [SSS 7.0±7.2 vs 1.9±3.1 ($p<0.001$), SRS 2.5±6.1 vs 0.5±1.4 ($p=0.008$) and SDS 4.3±3.5 vs 1.3±2.2 ($p<0.001$)]. The SRS was significantly higher in patients with fixed perfusion defects than in those without fixed perfusion defects [4.4±8.1 vs 0.5±1.4 ($p<0.001$)]. Similarly, SDS was elevated in patients with reversible perfusion defects compared to those without reversible perfusion defects [5.0±4.4 vs 1.4±2.2 ($p<0.001$)].

Comparison of 64-slice CTA and MPI

Per coronary artery analysis

Four of the 23 excluded coronary arteries were associated with perfusion defects of corresponding territories on MPI (four fixed perfusion defects) that had to be excluded from per artery analysis.

Figure 4 shows an overview of morphological and functional findings. Applying a cut-off for area stenoses of 50%, 17 (29.8%) of 57 stenotic main coronary arteries
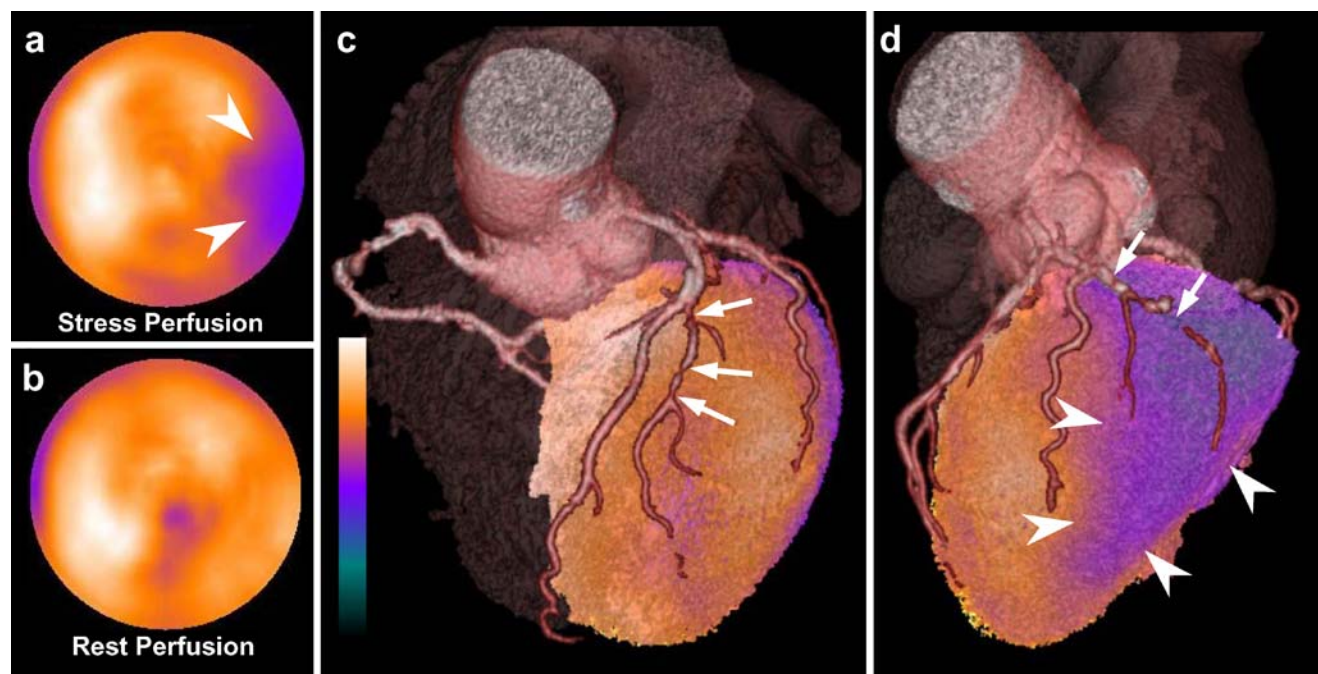

Fig. 2 a, b Semiquantitative polar maps of perfusion during vasodilator stress (a) and at rest (b), showing a reversible perfusion defect at the lateral base (*arrowheads*). For presentation purposes, functional (MPI) and morphological (CTA) information was fused, generating three-dimensional (3D) volume-rendered SPECT/CT images. c Anterior view of fused 3D SPECT-CT images showing serial lesions of the prominent first diagonal branch (*arrows*) which are not haemodynamically relevant. d The lateral view shows a subtotal or total occlusion of the mid LCX (*arrows*) and the corresponding ischaemia (*arrowheads*) matching the territory of the LCX
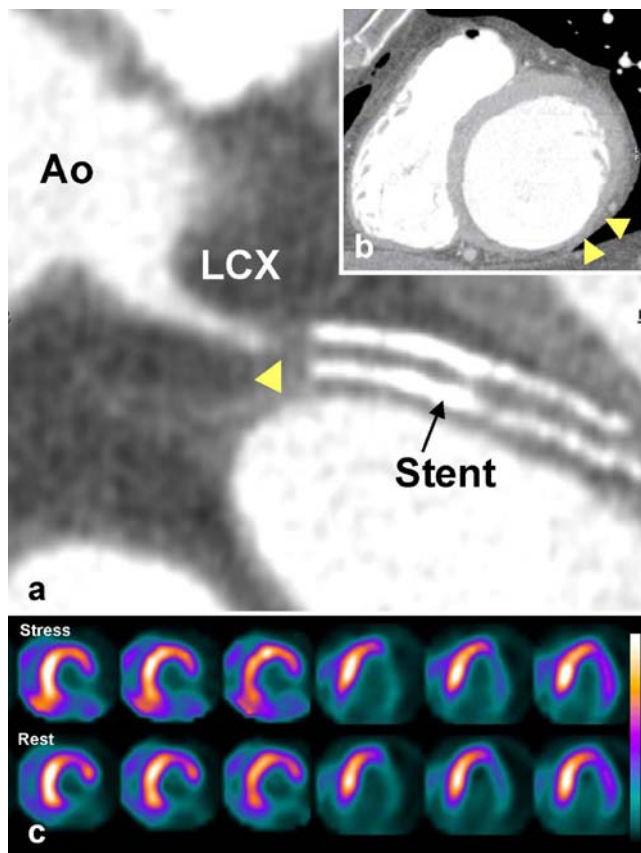
Fig. 3 **a** Curved two-dimensional reformatted 64-slice CT image of the LCX arising from the aorta (*Ao*) with complete occlusion proximal to the stent (*arrowhead*). **b** Multiplanar reformatted CT image in the two-chamber short axis view, showing a thinned inferolateral myocardium (*arrowheads*) correlating with the perfusion defect on MPI images. **c** Short-axis (*left*) and horizontal long axis (*right*) slices of MPI stress and rest images obtained with ^{99m}Tc-tetrofosmin revealing a large fixed inferolateral perfusion defect

were associated with a perfusion defect in its corresponding territory on MPI (11 reversible and six fixed defects). Thirty-nine (68.4%) of 57 stenotic main coronary arteries were not associated with any perfusion defect on MPI, and in one case (1.8%) the stenotic coronary artery did not correspond to the perfusion defect on MPI. Three patients showed perfusion defects on MPI without corresponding stenoses on CTA (two fixed and one reversible defect).

For coronary stenoses ≥75% we found that 16 (50.0%) of 32 stenotic main vessels on 64-slice CTA were associated with a perfusion defect in the corresponding territory on MPI (ten reversible and six fixed perfusion defects) (Fig. 4). Of the remaining 344 coronary arteries, only five were associated with a perfusion defect on MPI (two being reversible and three, fixed).

The sensitivity, specificity, NPV, PPV and accuracy of CTA for the prediction of any perfusion defects and of reversible defects only on MPI are given in Table 2, for coronary stenoses ≥50% and ≥75%.

Of the 25 intermediate stenoses (50–75% area stenosis), only one was associated with a (reversible) perfusion defect on MPI, while 24 proved functionally irrelevant on MPI.

Per patient analysis

Nine of 100 patients were excluded from per patient analysis because of heavy calcifications or significant motion artefacts on CTA. Three of these patients had a total of four fixed perfusion defects. Patients who had segments that could not be reliably assessed but had significant stenoses in another segment of the same coronary artery were not excluded from per patient analysis as they were correctly diagnosed as having CAD.

Figure 5 shows an overview of morphological and functional findings. For coronary stenoses ≥50%, we found that 18 (50.0%) of the 36 patients with stenotic main vessels on 64-slice CTA had perfusion defects on MPI. One patient had both a fixed and a reversible perfusion defect, six patients had a fixed perfusion defect and 11 patients had a reversible perfusion defect. Of the 55 patients without significant stenoses on CTA, two had a perfusion defect on MPI (one fixed and one reversible). The remaining 53 patients showed no perfusion defects on MPI.

Applying a cut-off of ≥75%, we found that 15 (68.2%) of 22 patients with stenotic main vessels on CTA had perfusion defects on MPI (nine reversible, five fixed and one patient with both reversible and fixed perfusion defects) (Fig. 5). Of the remaining 69 patients, five had a perfusion defect on MPI (three being reversible and two, fixed).

The sensitivity, specificity, NPV, PPV and accuracy of CTA for the prediction of any perfusion defects and of reversible defects only on MPI, on a per patient basis, are given in Table 3, for coronary stenoses ≥50% and ≥75%.

Discussion

Our study documents an excellent ability of 64-slice CTA to rule out functionally relevant CAD as indicated by the high NPV in a population with intermediate pretest likelihood. This high NPV was not affected by the two different cut-offs for coronary stenoses chosen in this study (50% or 75% area stenosis). However, an abnormal 64-slice CTA is a poor predictor of functionally relevant coronary stenoses. When shifting the cut-off value from 50% to 75% area stenosis, the low PPV showed only a modest increase. Patients with positive CTA need further evaluation for obstructive CAD and will possibly undergo invasive CA although only about half of these patients will have obstructive CAD. The results of our study underline the value of a combined assessment of ischaemia (MPI) and anatomical lesion (CTA) since a substantial proportion of
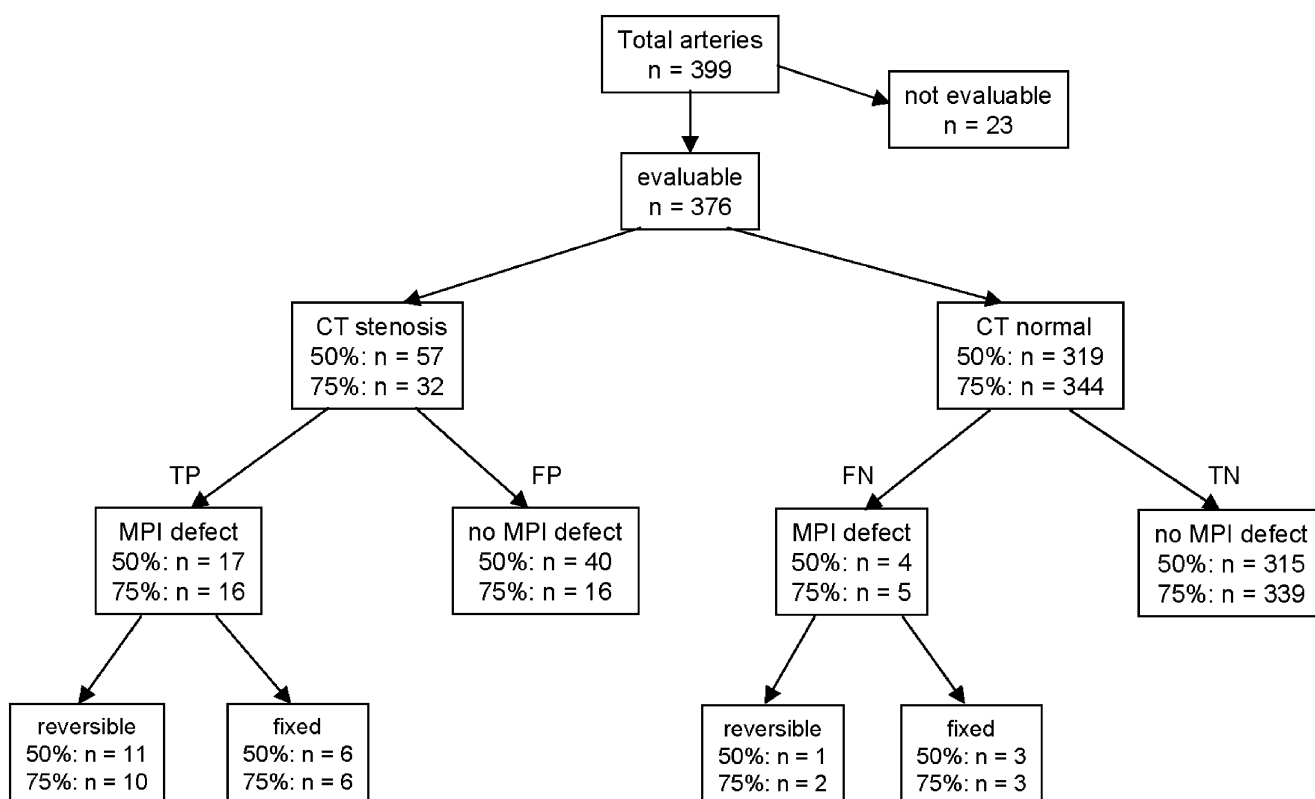
Fig. 4 Overview of morphological and functional findings per coronary artery (50% and 75% area stenosis). *TP* true positives, *FP* false positives, *FN* false negatives, *TN* true negatives

patients did not qualify for a coronary intervention as indicated by the absence of significant ischaemia on MPI, while CTA revealed subclinical lesions where risk factor modification may be beneficial.

The low PPV of 64-slice CTA for the detection of functionally relevant stenoses in our study appears to be at variance with the reported excellent diagnostic accuracy for CTA compared with conventional CA. Several studies validating CTA with a 16-slice CT scanner versus CA reported an overall sensitivity and specificity of 72–95% and 86–98%, respectively [5–8]. Recently, use of 64-slice CTA with faster gantry rotation and enhanced spatial and temporal resolution was shown to yield a further improvement in diagnostic accuracy (sensitivity 80–99%, specificity 91–97%) compared with the 16-detector systems [9–13]. However, in those studies CTA was validated against CA, both being imaging tools that rely on the assessment of coronary lumen.

By contrast, the aim of the present study was to evaluate the diagnostic accuracy of 64-slice CTA in predicting the functional relevance of coronary stenoses, which is a valuable prognostic factor with important implications for clinical decision making [15]. Despite significant advances in CA, the definition of a functionally relevant stenosis on

Table 2 Accuracy of 64-slice CTA in the detection of perfusion defects in corresponding target areas on MPI

	Sens (%)	Spec (%)	NPV (%)	PPV (%)	Acc (%)
≥50% stenosis					
Any perfusion defect	81	89	99	30	88
Reversible perfusion defects only	92	87	100	19	88
≥75% stenosis					
Any perfusion defect	76	95	99	50	94
Reversible perfusion defects only	83	94	99	31	94

Per artery analysis (*n*=399)

p=NS for comparison between stenoses ≥50% and ≥75%

Sens sensitivity, *Spec* specificity, *NPV* negative predictive value, *PPV* positive predictive value, *Acc* accuracy. *Any perfusion defect* = fixed, reversible or mixed defects
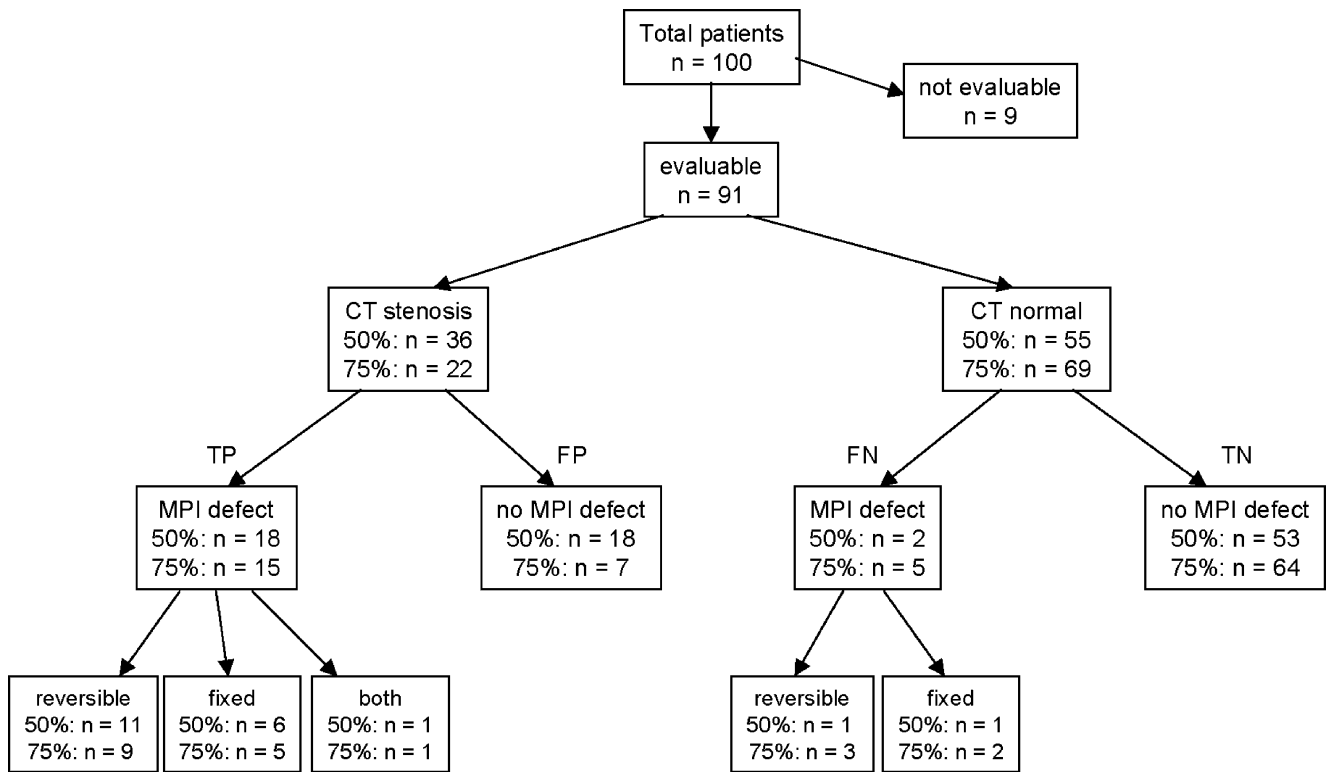
Fig. 5 Overview of morphological and functional findings per patient (50% and 75% area stenosis). *TP* true positives, *FP* false positives, *FN* false negatives, *TN* true negatives

the basis of purely morpho-anatomical criteria remains controversial [20, 34]. Many factors that cannot be fully and correctly evaluated by CA will eventually determine whether or not a given lesion produces stress-induced ischaemia, and therefore prior functional assessment by stress ECG or MPI is generally recommended [15]. The low PPV found in our study is in line with a previous report by Hacker and co-workers [4] in 25 patients, where the NPV and PPV of 16-slice CTA for the detection of functionally relevant stenoses were 96% and 47%, respectively. In contrast to the latter study, we used quantitative analysis of MPI and CTA. In addition, our larger study population allowed the clinically more relevant per patient

analysis to be conducted. Our results support the notion that no matter how accurate CTA may become with future technical refinements, the two pieces of information provided by MPI and luminology are hard to compare, this being inherent to the duality of morphological versus functional testing. While Hacker et al. set their cut-off at 50% area stenosis, a diameter stenosis of 50% (corresponding to 75% area stenosis) is more commonly accepted as a reasonable cut-off for clinical relevance. This has been substantiated by a quantitative myocardial perfusion study with positron emission tomography (PET) showing a progressive decline in flow reserve for lesions above 75% area stenosis [35], though the large scatter

Table 3 Accuracy of 64-slice CTA in the detection of perfusion defects in corresponding target areas on MPI

	Sens (%)	Spec (%)	NPV (%)	PPV (%)	Acc (%)
≥50% stenosis					
Any perfusion defect	90	75	96	50	78
Reversible perfusion defects only	92	68	98	31	72
≥75% stenosis					
Any perfusion defect	75	90	93	68	87
Reversible perfusion defects only	64	83	93	41	80

Per patient analysis ($n=100$)
p=NS for comparison between stenoses ≥50% and ≥75%
Sens sensitivity, *Spec* specificity, *NPV* negative predictive value, *PPV* positive predictive value, *Acc* accuracy. *Any perfusion defect* = fixed, reversible or mixed defects

prevents general extrapolation and warrants individual perfusion scanning. Thus, applying a cut-off value of 50% area stenosis allows CTA to accurately rule out lesions with functional significance as confirmed by MPI. This high NPV, however, is accomplished at the cost of a low PPV, as many stenoses slightly above 50% may not induce ischaemia and will account for the high false positive number. Accordingly, when shifting the cut-off value from 50% to 75% area stenosis, the PPV tended to improve without any drop in NPV (p=NS).

Despite the reported accuracy of 64-slice CTA, the image quality of CTA is impaired by motion artefacts in the presence of high heart rates or arrhythmia. Particularly the RCA exhibits large motion amplitudes and is commonly associated with significant motion artefacts affecting image quality [36]. The introduction of new CT systems with 64 detector rows, faster gantry rotation and improved temporal resolution has substantially reduced motion artefacts. In fact, while Hacker et al. [4] reported 30% of coronary segments to be uninterpretable when using a 16-detector scanner, we excluded only 6.1% of segments. In addition, coronary arteries with heavy calcifications are not easily amenable to reliable quantification of the degree of stenosis owing to significant blooming artefacts obscuring the vascular lumen. The substantially lower CCS of 231 in the population studied by Mollet et al. [12] might have contributed to their lower exclusion rate compared to our population with a CCS of 505.

Study limitations

In the present study no CA was available to verify the CTA findings, although CA has remained the gold standard for coronary anatomy. Instead, the aim of the study was to assess the impact of CTA findings on perfusion. Therefore, MPI was used as the gold standard.

There are also shortcomings to using SPECT MPI as the gold standard for functionally relevant coronary stenoses. SPECT MPI has a high sensitivity for detecting significant coronary stenoses, but specificity is somewhat lower [15]. Additionally, SPECT MPI is a technically demanding procedure that is susceptible to a variety of artefacts, particularly attenuation artefacts due to diaphragmatic attenuation. However, considering the extensive experience accumulated over two decades, including the prognostic information provided by SPECT MPI, this technique can be regarded as being the best evaluated and best established non-invasive imaging tool for the functional assessment of known or suspected CAD. Moreover, the use of X-ray-based attenuation correction and information from gated SPECT—as performed in our patients—is known to improve the specificity of SPECT MPI studies without affecting the sensitivity [15].

Furthermore, there are important shortcomings to quantitative assessment of coronary stenoses on CTA. In comparison with QCA, quantitative CTA is restricted by an inferior spatial resolution particularly in small vessels <1.5 mm. However, Raff and co-workers [9] demonstrated a good correlation of QCA and quantitative CTA using the same technique as was used in our study.

In order to reduce radiation exposure, prospective tube current modulation was used in all patients. This technique allows a reduction in radiation exposure of approximately 50% but precludes the use of end-systolic phases for coronary reconstruction in cases of arrhythmia [12].

Finally, as the majority of the study population were males, not all the conclusions may be extrapolated to female populations.

Clinical implications

Sixty-four-slice CTA is a reliable tool for identifying patients without functionally relevant CAD in a non-selected population with intermediate pretest likelihood. However, an abnormal CTA is a poor predictor of ischaemia and it remains to be determined whether the risks inherent with unnecessary invasive diagnostic angiography may be offset by the number of invasive procedures prevented by the negative results on CTA. It appears that the technique should be used in low to intermediate likelihood patients to exclude CAD rather than to define the exact extent of CAD. On the other hand, a normal MPI does not exclude the presence of subclinical CAD for which aggressive cardiovascular risk modification may be warranted.

References

1. Cook S, Togni M, Walpoth N, Maier W, Muehlberger V, Legrand V, et al. Percutaneous coronary interventions in Europe 1992–2003. EuroIntervention 2006;1:374–9.
2. Achenbach S, Daniel WG. Noninvasive coronary angiography—an acceptable alternative? N Engl J Med 2001;345:1909–10.
3. Achenbach S, Ulzheimer S, Baum U, Kachelriess M, Ropers D, Giesler T, et al. Noninvasive coronary angiography by retrospectively ECG-gated multislice spiral CT. Circulation 2000;102:2823–8.
4. Hacker M, Jakobs T, Matthiesen F, Vollmar C, Nikolaou K, Becker C, et al. Comparison of spiral multidetector CT angiography and myocardial perfusion imaging in the noninvasive detection of functionally relevant coronary artery lesions: first clinical experiences. J Nucl Med 2005;46:1294–300.

5. Nieman K, Cademartiri F, Lemos PA, Raaijmakers R, Pattynama PM, de Feyter PJ. Reliable noninvasive coronary angiography with fast submillimeter multislice spiral computed tomography. Circulation 2002;106:2051–4.

6. Mollet NR, Cademartiri F, Nieman K, Saia F, Lemos PA, McFadden EP, et al. Multislice spiral computed tomography coronary angiography in patients with stable angina pectoris. J Am Coll Cardiol 2004;43:2265–70.

7. Kuettner A, Beck T, Drosch T, Kettering K, Heuschmid M, Burgstahler C, et al. Diagnostic accuracy of noninvasive coronary imaging using 16-detector slice spiral computed tomography with 188 ms temporal resolution. J Am Coll Cardiol 2005;45:123–7.

8. Mollet NR, Cademartiri F, Krestin GP, McFadden EP, Arampatzis CA, Serruys PW, et al. Improved diagnostic accuracy with 16-row multi-slice computed tomography coronary angiography. J Am Coll Cardiol 2005;45:128–32.

9. Raff GL, Gallagher MJ, O'Neill WW, Goldstein JA. Diagnostic accuracy of noninvasive coronary angiography using 64-slice spiral computed tomography. J Am Coll Cardiol 2005;46:552–7.

10. Leschka S, Alkadhi H, Plass A, Desbiolles L, Grunenfelder J, Marincek B, et al. Accuracy of MSCT coronary angiography with 64-slice technology: first experience. Eur Heart J 2005;26:1482–7.

11. Leber AW, Knez A, von Ziegler F, Becker A, Nikolaou K, Paul S, et al. Quantification of obstructive and nonobstructive coronary lesions by 64-slice computed tomography: a comparative study with quantitative coronary angiography and intravascular ultrasound. J Am Coll Cardiol 2005;46:147–54.

12. Mollet NR, Cademartiri F, van Mieghem CA, Runza G, McFadden EP, Baks T, et al. High-resolution spiral computed tomography coronary angiography in patients referred for diagnostic conventional coronary angiography. Circulation 2005;112:2318–23.

13. Pugliese F, Mollet NR, Runza G, van Mieghem C, Meijboom WB, Malagutti P, et al. Diagnostic accuracy of non-invasive 64-slice CT coronary angiography in patients with stable angina pectoris. Eur Radiol 2005;1–8.

14. Namdar M, Hany TF, Koepfli P, Siegrist PT, Burger C, Wyss CA, et al. Integrated PET/CT for the assessment of coronary artery disease: a feasibility study. J Nucl Med 2005;46:930–5.

15. Klocke FJ, Baird MG, Lorell BH, Bateman TM, Messer JV, Berman DS, et al. ACC/AHA/ASNC guidelines for the clinical use of cardiac radionuclide imaging—executive summary: a report of the American College of Cardiology/American Heart Association Task Force on Practice Guidelines (ACC/AHA/ASNC Committee to Revise the 1995 Guidelines for the Clinical Use of Cardiac Radionuclide Imaging). J Am Coll Cardiol 2003;42:1318–33.

16. Iskander S, Iskandrian AE. Risk assessment using single-photon emission computed tomographic technetium-99m sestamibi imaging. J Am Coll Cardiol 1998;32:57–62.

17. Beller GA, Zaret BL. Contributions of nuclear cardiology to diagnosis and prognosis of patients with coronary artery disease. Circulation 2000;101:1465–78.

18. Brown KA, Altland E, Rowen M. Prognostic value of normal technetium-99m-sestamibi cardiac imaging. J Nucl Med 1994;35:554–7.

19. Hachamovitch R, Berman DS, Shaw LJ, Kiat H, Cohen I, Cabico JA, et al. Incremental prognostic value of myocardial perfusion single photon emission computed tomography for the prediction of cardiac death: differential stratification for risk of cardiac death and myocardial infarction. Circulation 1998;97:535–43.

20. Topol EJ, Nissen SE. Our preoccupation with coronary luminology. The dissociation between clinical and angiographic findings in ischemic heart disease. Circulation 1995;92:2333–42.

21. Pavin D, Delonca J, Siegenthaler M, Doat M, Rutishauser W, Righetti A. Long-term (10 years) prognostic value of a normal thallium-201 myocardial exercise scintigraphy in patients with coronary artery disease documented by angiography. Eur Heart J 1997;18:69–77.

22. Schepis T, Gaemperli O, Koepfli P, Valenta I, Strobel K, Brunner A, et al. Comparison of 64-slice CT with gated SPECT for evaluation of left ventricular function. J Nucl Med 2006;47:1288–94.

23. Cerqueira MD, Verani MS, Schwaiger M, Heo J, Iskandrian AS. Safety profile of adenosine stress perfusion imaging: results from the Adenoscan Multicenter Trial Registry. J Am Coll Cardiol 1994;23:384–9.

24. Koepfli P, Hany TF, Wyss CA, Namdar M, Burger C, Konstantinidis AV, et al. CT attenuation correction for myocardial perfusion quantification using a PET/CT hybrid scanner. J Nucl Med 2004;45:537–42.

25. Fricke H, Fricke E, Weise R, Kammeier A, Lindner O, Burchert W. A method to remove artifacts in attenuation-corrected myocardial perfusion SPECT introduced by misalignment between emission scan and CT-derived attenuation maps. J Nucl Med 2004;45:1619–25.

26. Germano G, Kavanagh PB, Waechter P, Areeda J, Van Kriekinge S, Sharir T, et al. A new algorithm for the quantitation of myocardial perfusion SPECT. I: Technical principles and reproducibility. J Nucl Med 2000;41:712–9.

27. Berman DS, Kiat H, Friedman JD, Wang FP, van Train K, Matzer L, et al. Separate acquisition rest thallium-201/stress technetium-99m sestamibi dual-isotope myocardial perfusion single-photon emission computed tomography: a clinical validation study. J Am Coll Cardiol 1993;22:1455–64.

28. Schepis T, Gaemperli O, Koepfli P, Ruegg C, Burger C, Leschka S, et al. Use of coronary calcium score scans from stand-alone multislice computed tomography for attenuation correction of myocardial perfusion SPECT. Eur J Nucl Med Mol Imaging 2007;34:11–9.

29. Giesler T, Baum U, Ropers D, Ulzheimer S, Wenkel E, Mennicke M, et al. Noninvasive visualization of coronary arteries using contrast-enhanced multidetector CT: influence of heart rate on image quality and stenosis detection. AJR Am J Roentgenol 2002;179:911–6.

30. Shim SS, Kim Y, Lim SM. Improvement of image quality with beta-blocker premedication on ECG-gated 16-MDCT coronary angiography. AJR Am J Roentgenol 2005;184:649–54.

31. Hoffmann MH, Shi H, Manzke R, Schmid FT, De Vries L, Grass M, et al. Noninvasive coronary angiography with 16-detector row CT: effect of heart rate. Radiology 2005;234:86–97.

32. Austen WG, Edwards JE, Frye RL, Gensini GG, Gott VL, Griffith LS, et al. A reporting system on patients evaluated for coronary artery disease. Report of the Ad Hoc Committee for Grading of Coronary Artery Disease, Council on Cardiovascular Surgery, American Heart Association. Circulation 1975;51:5–40.

33. Obuchowski NA. Receiver operating characteristic curves and their use in radiology. Radiology 2003;229:3–8.

34. White CW, Wright CB, Doty DB, Hiratza LF, Eastham CL, Harrison DG, et al. Does visual interpretation of the coronary arteriogram predict the physiologic importance of a coronary stenosis? N Engl J Med 1984;310:819–24.

35. Uren NG, Melin JA, De Bruyne B, Wijns W, Baudhuin T, Camici PG. Relation between myocardial blood flow and the severity of coronary-artery stenosis. N Engl J Med 1994;330:1782–8.

36. Lu B, Mao SS, Zhuang N, Bakhsheshi H, Yamamoto H, Takasu J, et al. Coronary artery motion during the cardiac cycle and optimal ECG triggering for coronary artery imaging. Invest Radiol 2001;36:250–6.